trast in the shallow mantle close to 32°N. There is no contradiction, however, because these phases propagate in a different direction, that is, horizontally instead of subvertically, and are primarily sensitive to mantle velocities immediately beneath the Moho, whereas the tomographic inversion can only recover velocities vertically averaged over 100-km depth range because of its limited resolving power. A possible interpretation of the high velocities could be that they represent the front of a detaching mantle lithosphere, where the wedge thus formed is filled by warmer mantle from the north. The wedge is too thin to be seen in teleseismic tomography but accounts for the southward extent of low P_n velocities and strong S_n attenuation as well as the dispersion of intermediate-period surface waves.

References and Notes

1. A. Yin, T. M. Harrison, *Annu. Rev. Earth Planet. Sci.* **28**, 211 (2000).
2. C. M. Powell, P. G. Conaghan, *Earth Planet. Sci. Lett.* **20**, 1 (1973).
3. G. Brandon, B. Romanowicz, *J. Geophys. Res.* **91**, 6547 (1986).
4. A. Curtis, J. H. Woodhouse, *J. Geophys. Res.* **102**, 11789 (1997).
5. A. J. Rodgers, S. Y. Schwartz, *J. Geophys. Res.* **103**, 7137 (1998).
6. R. Rapine, F. Tilmann, M. West, J. Ni, A. Rodgers, *J. Geophys. Res.* **108**, 2120, 10.1029/2001JB000445 (2003).
7. M. Barazangi, J. Ni, *Geology* **10**, 179 (1982).
8. D. McNamara, W. Walter, T. Owens, C. Ammon, *J. Geophys. Res.* **102**, 493 (1997).
9. M. R. W. Johnson, *Earth Sci. Rev.* **59**, 101 (2002).
10. P. G. DeCelles, D. M. Robinson, G. Zandt, *Tectonics* **21**, 10.1029/2001TC001322 (2002).
11. Q. Wang *et al.*, *Science* **294**, 574 (2001).
12. Further details of the travel-time picking and tomographic inversion can be found in the supporting online material (SOM).
13. The resolution power of the data set was estimated by evaluating selected columns of the resolution matrix and by carrying out inversions with synthetic travel times for realistic models.
14. R. Zhou, S. P. Grand, F. Tajima, X.-Y. Ding, *Geophys. Res. Lett.* **23**, 25 (1996).
15. G. Wittlinger *et al.*, *Earth Planet. Sci. Lett.* **139**, 263 (1996).
16. R. Kind *et al.*, *Science* **298**, 1219 (2002).
17. S.-I. Karato, *Geophys. Res. Lett.* **20**, 1623 (1993).
18. S. Turner *et al.*, *Nature* **364**, 50 (1993).
19. H. Sato, I. S. Sacks, T. Murase, *J. Geophys. Res.* **94**, 5689 (1989).
20. G. Hirth, D. L. Kohlstedt, *Earth Planet. Sci. Lett.* **144**, 93 (1996).
21. P. Tapponnier *et al.*, *Science* **294**, 1671 (2001).
22. D. McNamara, E., T. Owens, P. Silver, F. Wu, *J. Geophys. Res.* **99**, 13655 (1994).
23. W.-C. Huang *et al.*, *J. Geophys. Res.* **105**, 27979 (2000).
24. W. P. Chen, S. Özalaybey, *Geophys. J. Int.* **135**, 93 (1998).
25. P. Bird, *J. Geophys. Res.* **83**, 4957 (1978).
26. A. M. Marotta, M. Fernandez, R. Sabadini, *Geophys. J. Int.* **139**, 98 (1999).
27. C. P. Conrad, *Geophys. J. Int.* **143**, 52 (2000).
28. A. Chemenda, J.-P. Burg, M. Mattauer, *Earth Planet. Sci. Lett.* **174**, 397 (2000).
29. C. J. Allègre *et al.*, *Nature* **307**, 17 (1984).

30. Project INDEPTH III was supported by the Ministry of Land and Resources of the People's Republic of China, the U.S. National Science Foundation Continental Dynamics Program (grant EAR 9614616), and the Deutsche Forschungsgemeinschaft and GeoForschungsZentrum Potsdam (GFZ), Germany. F.T. thanks the Alexander von Humboldt Foundation for partial support of this work. We thank the Chinese scientists and the Tibetans for their help in the field. The instruments were provided by the IRIS-PASSCAL program and the GFZ instrument pool. We thank J. VanDecar for the initial version of the tomography code used; J. P. Morgan, C. Conrad, J. Jackson, K. Priestley, and R. Meissner for helpful discussions; and three anonymous reviewers for constructive reviews. This is Cambridge Department of Earth Sciences contribution number 7453.

Supporting Online Material

www.sciencemag.org/cgi/content/full/300/5624/1424/DC1
SOM Text
Figs. S1 to S6
Tables S1 to S3
References

27 January 2003; accepted 2 May 2003

Modulation of Phospholipid Signaling by GLABRA2 in Root-Hair Pattern Formation

Yohei Ohashi,[1] Atsuhiro Oka,[1] Renato Rodrigues-Pousada,[2] Marco Possenti,[2] Ida Ruberti,[3] Giorgio Morelli,[2] Takashi Aoyama[1]*

The root-hair pattern of *Arabidopsis* is determined through a regulatory circuit composed of transcription factor genes. The homeobox gene *GLABRA2* (*GL2*) has been considered a key component, acting farthest downstream in this regulation. GL2 modified to include a transactivating function caused epidermal cells to develop ectopic root hairs or root hair–like structures. With this system, the phospholipase Dζ1 gene (*AtPLDζ1*) was identified as a direct target of GL2. Inducible expression of *AtPLDζ1* promoted ectopic root-hair initiation. We conclude that GL2 exerts its regulatory effect on root-hair development through modulation of phospholipid signaling.

Cell morphogenesis and its disposition pattern are crucial for plants to ensure functional tissue and organ structures, particularly because the relative positions of plant cells do not change after proliferation. Root-hair formation provides a simple model system that allows exploration of the mechanisms that regulate both pattern formation and morphogenesis (*1*, *2*).

In *Arabidopsis*, the root epidermis is composed of two types of cell files, only one of which produces root hairs (Fig. 1A) (*3*). Each hair cell file makes contact with two adjacent, underlying, cortical cell files, whereas each hairless cell file makes contact with a single cortical cell file. Mutations in the *GLABRA2* (*GL2*) (*4*, *5*), *WEREWOLF* (*WER*) (*6*), and *TRANSPARENT TESTA GLABRA 1* (*TTG1*) (*7*) genes cause all the cell files in the root epidermis to develop root hairs. Conversely, mutations in *CAPRICE* (*CPC*) (*8*) reduce the frequency of root hairs in hair cell files. *GL2*, which encodes a homeodomain protein (*9*), is expressed predominantly in hairless cell files and is thought to be a negative regulator of root-hair development (*4*, *5*). Because the level of *GL2* transcription is decreased in *ttg1* mutant plants (*4*), TTG1 has been suggested to regulate *GL2* positively. *WER* and *CPC*, which encode Myb transcription factors (*6*, *8*) and cross-regulate each other in a feedback loop (*10*), positively and negatively regulate the position-specific expression of *GL2*, respectively (*6*, *10*). Although such a transcriptional regulatory circuit may be involved in determining root-hair pattern formation, subsequent events remain obscure. We have analyzed these downstream events by identifying genes affected by GL2, the transcription factor farthest downstream in the known feedback loop.

To increase the expression of GL2 target genes, we converted GL2 into a strong transcriptional activator by replacing its N-terminal acidic region with the transactivating domain of the herpes viral protein VP16. The modified GL2 gene (*VP16-GL2ΔN*) was expressed in transgenic plants under the control of the *GL2* promoter or of the glucocorticoid-inducible gene expression system GVG (*11*). In 16 of 21 independent transgenic lines carrying the *GL2* promoter–driven transgene, all the cell files in the root epidermis developed root hairs (Fig. 1, B and C), and hypocotyl epidermal cell files composed of relatively elongated cells developed root hair–like structures (Fig. 1, D and E). In plants with severe phenotypes, root hair–like structures were also observed on the abaxial surface of the hypocotyl/cotyledon junction

[1]Institute for Chemical Research, Kyoto University, Uji, Kyoto 611-0011, Japan. [2]Istituto Nazionale di Ricerca per gli Alimenti e la Nutrizione, Via Ardeatina 546, 00178 Rome, Italy. [3]Centro di studio per gli Acidi Nucleici, c/o Dipartimento di Genetica e Biologia Molecolare, Università di Roma La Sapienza, Piazzale Aldo Moro 5, 00185 Rome, Italy.

*To whom correspondence should be addressed. E-mail: aoyama@scl.kyoto-u.ac.jp

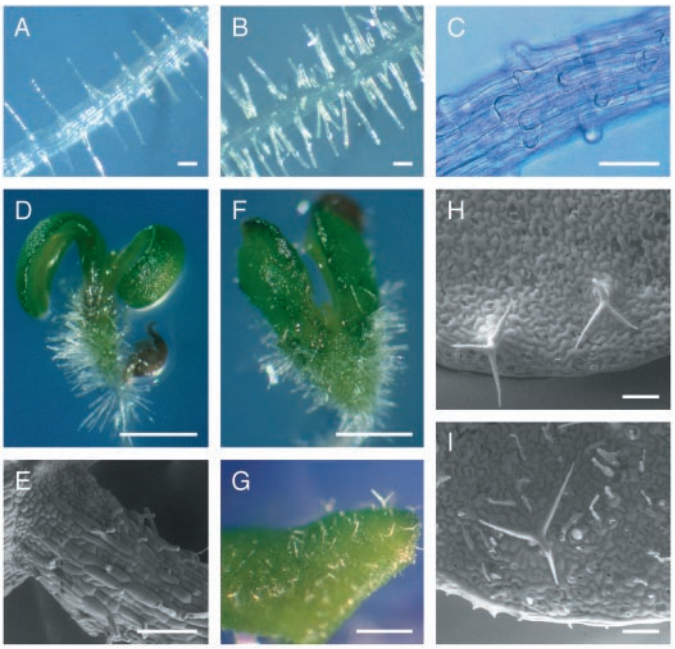

Fig. 1. Phenotypes of transgenic plants expressing *VP16-GL2ΔN*. (**A**) Root hairs of a wild-type plant. (**B** to **F**) Transgenic plants carrying the *GL2* promoter–driven *VP16-GL2ΔN* gene. (B) Root hairs. (C) Root-hair bulges. [(D) to (F)] Root hair–like structures on the surface of [(D) and (E)] hypocotyls and (F) the hypocotyl/cotyledon junction. (**G** to **I**) The leaf surfaces of (H) DEX-untreated and [(G) and (I)] DEX-treated transgenic plants carrying the GVG-inducible *VP16-GL2ΔN* gene. Scanning electron microscope images are shown in (E), (H), and (I). Scale bars, 100 μm [(A) to (C), (E), (H), and (I)], 1 mm [(D), (F), and (G)].

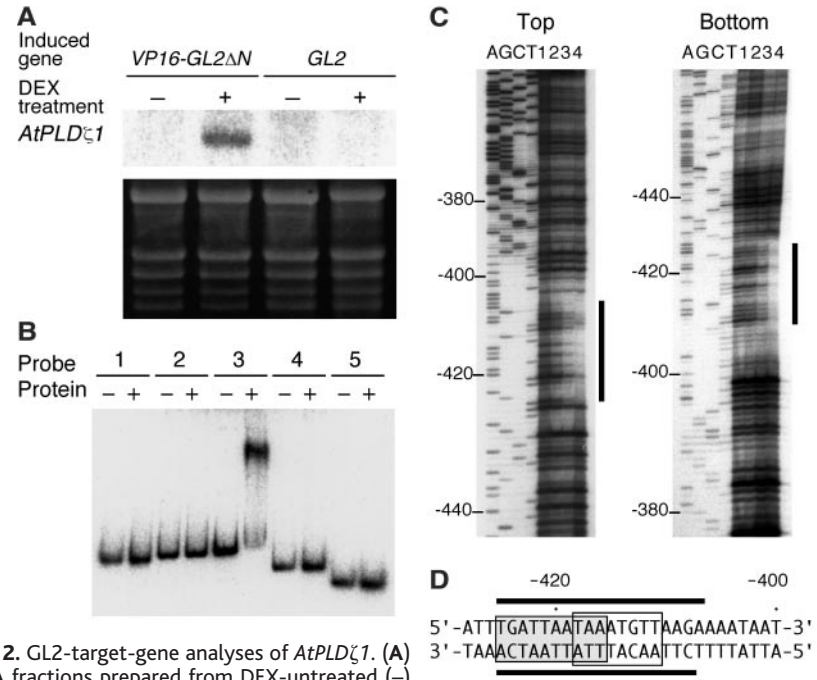

Fig. 2. GL2-target-gene analyses of *AtPLDζ1*. (**A**) RNA fractions prepared from DEX-untreated (–) or DEX-treated (+) transgenic plants that carried the GVG-inducible *VP16-GL2ΔN* or *GL2* genes were subjected to Northern analysis with a probe specific for *AtPLDζ1*. The same RNA fractions were electrophoresed on an agarose gel and stained with ethidium bromide. (**B**) A gel mobility shift analysis was performed, with the truncated GL2 protein (amino acids 1 to 235) that contained the HD-ZIP domain and upstream DNA fragments of *AtPLDζ1*. The DNA regions used were probes 1 (–1079 to –855), 2 (–878 to –654), 3 (–653 to –351), 4 (–350 to –141), and 5 (–140 to –1); the negative numbers in parentheses indicate the number of base pairs upstream from the AtPLDζ1 initiation codon. Each DNA fragment (0.1 pmol) was end-labeled, incubated without (–) or with (+) the truncated protein (1.8 pmol), and fractionated on a polyacrylamide gel. (**C**) DNase I footprints of the top and bottom strands of probe 3 were generated with the truncated GL2 protein. The amount of protein added to the DNA fragment (0.02 pmol) was 0.0, 0.4, 1.8, and 5.4 pmol for lanes 1, 2, 3, and 4, respectively. Lanes A, G, C, and T are reference sequence ladders. The regions protected from DNase I are indicated by bars. (**D**) Protected regions in the DNase I footprint analysis are indicated by bars along the double-stranded sequences. The shaded and open boxes indicate a pseudopalindromic sequence and a sequence similar to the L1-box [5′-TAAATG(C/T)A-3′] (*16*), respectively.

(Fig. 1F). The cells that underwent these morphological changes were some of those with *GL2* promoter activity (*5*, *12*). Transgenic plants carrying the GVG-inducible *VP16-GL2ΔN* gene grew normally in the absence of dexamethasone (DEX), a glucocorticoid derivative (Fig. 1H). After their leaves were soaked in DEX solution, a population of leaf epidermal cells changed shape and developed protruding root hair–like structures in 10 of 13 independent lines obtained (Fig. 1, G and I).

We histochemically examined these transgenic plants for promoter activity of the expansin 7 gene (*At-EXP7*), which is expressed specifically in root-hair cells (*13*), using a β-glucuronidase (GUS) reporter gene. *At-EXP7* promoter activity was found in cells that bore ectopic root hairs and root hair–like structures (fig. S1), suggesting that those cells had undergone the same developmental processes as root-hair cells. Neither root hair–like structures nor ectopic *At-EXP7* promoter activity was observed when a gene that encoded the authentic GL2 protein was inducibly expressed by the GVG system (*14*).

We conducted a subtraction experiment using cDNAs prepared from DEX-treated plants that carried the GVG-inducible *VP16-GL2ΔN* and the GVG-inducible *GL2* as tester and driver, respectively. In this experiment, we expected to detect GL2 target genes promoting root-hair development, because VP16-GL2ΔN and GL2 were thought to promote and repress root-hair development, respectively. From expression patterns of cloned subtracted cDNAs, we identified a clone that was specifically expressed in DEX-treated plants that carried the inducible *VP16-GL2ΔN* (Fig. 2A). The clone encoded a phospholipase D (PLD) named AtPLDζ1 (*15*).

We examined the physical interaction between the *AtPLDζ1* promoter and the GL2 DNA-binding domain in vitro. In a gel mobility shift analysis, a truncated GL2 protein containing the homeodomain-leucine-zipper (HD-ZIP) region was specifically bound to a 303-base pair (bp)–long DNA fragment, 350 bp upstream from the AtPLDζ1 initiation codon (Fig. 2B). Deoxyribonuclease I (DNase I) footprinting analysis revealed that the protein protected an 18-bp sequence in the fragment from DNase I (Fig. 2C). This sequence has two noticeable features (Fig. 2D): a pseudopalindromic structure and a sequence similar to that of the L1-box (*16*). The existence of the pseudopalindromic structure is consistent with the fact that the leucine-zipper of GL2 can mediate homodimerization (*4*). The L1-box is reported to be bound to ATML1, a homeodomain protein belonging to the HD-ZIP IV subfamily along with GL2 (*16*). These results indicate that GL2 recognizes promoter sequences of, and hence directly regulates, the *AtPLDζ1* gene.

To obtain in vivo evidence that GL2 regulates *AtPLDζ1* in root epidermal cells, we

examined the promoter activity of an *AtPLDζ1* upstream region that encompassed the GL2-binding sequence with a GUS histochemical analysis. Transgenic plants carrying the reporter gene showed GUS activity in various loci, including meristematic and vascular tissues (*14*). In developing wild-type root epidermis, GUS activity was higher in hair cell files than in hairless cell files (Fig. 3A). On the other hand, under the *gl2* mutant genetic background, both cell files showed the same level of GUS activity (Fig. 3B). A mutant reporter gene, of which the promoter contains substitutions at four base pairs in the sequence bound to the GL2 DNA-binding domain, conferred the same level of GUS activity to both cell files in wild-type root epidermis (Fig. 3C). These expression patterns indicated that GL2 represses the target gene in the development of hairless cells through the recognition sequence.

To investigate the function of AtPLDζ1 in root-hair development, we examined its tentative intracellular localization using a fusion protein of AtPLDζ1 and green fluorescent protein (GFP). In the transgenic root epidermis, fluorescence was observed mainly in the cell cortical region and showed a pattern suggesting the protein was localized in vesicles (Fig. 3, D to G). At early stages of root-hair development, the fusion protein was localized preferentially around bulges (Fig. 3, D and E). During growth of root hairs, relatively strong fluorescence was often observed around the root-hair apex (Fig. 3G). Next, we inducibly expressed *AtPLDζ1* using the GVG system. In the absence of DEX, the transgenic plants grew normally and had the same root surface structure as wild-type plants (Fig. 4B). After soaking the root surface in DEX solution, various abnormalities in root-hair development were observed in all nine transgenic lines obtained. In hair cells at stages after bulge formation, root hairs were frequently branched and swollen (Fig. 4, A, D, and E). At early stages, the DEX treatment induced bulges in all cell files (Fig. 4C) and sometimes numerous bulges on a single cell (Fig. 4F). These abnormalities were not observed in DEX-treated transgenic plants that carried a GVG-inducible luciferase gene (*14*). Thus AtPLDζ1 is likely involved in both initiation and maintenance of root-hair morphogenesis. Branched root hairs with shapes similar to that in Fig. 4E were frequently observed in *gl2* mutant

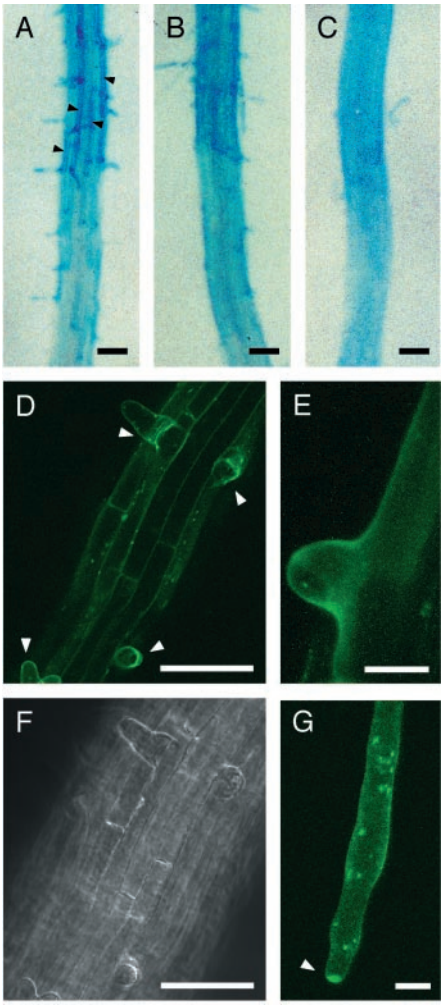

Fig. 3. Analyses of *AtPLDζ1* expression in transgenic plants. (**A** to **C**) Activity of the [(A) and (B)] wild-type and (C) mutant *AtPLDζ1* promoters in the root epidermis was analyzed histochemically with a GUS reporter gene under the [(A) and (C)] wild-type and (B) *gl2-5* mutant (*21*) genetic backgrounds. The arrowheads in (A) indicate root-hair cell files. (**D** to **G**) The intracellular localization of AtPLDζ1-GFP fusion protein, which was expressed under the control of the *AtPLDζ1* promoter. [(D), (E), and (G)] Fluorescence from the fusion protein was observed with confocal laser scanning microscopy. The arrowheads indicate relatively strong fluorescence signals around (D) bulges and (G) the root-hair apex. (F) A transparent light image of the root in (D). Scale bars: 100 μm [(A) to (D) and (F)], 10 μm [(E) and (G)].

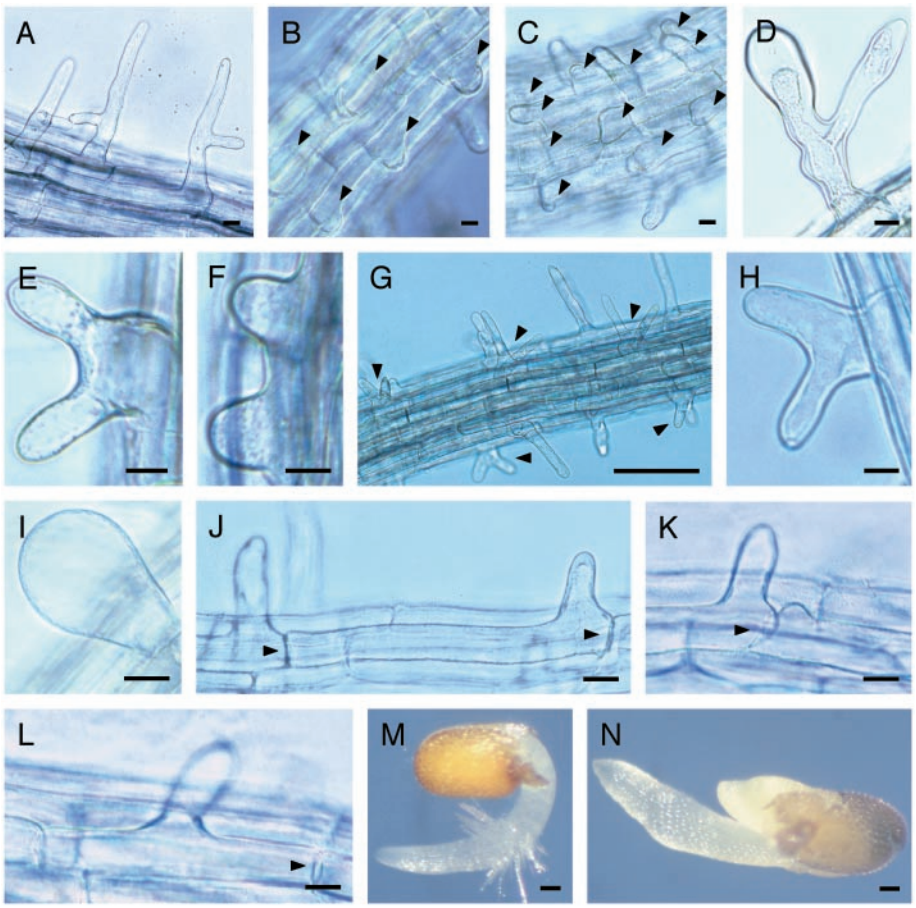

Fig. 4. Abnormalities in root hairs caused by increased and decreased levels of *AtPLDζ1* expression, a *gl2*-mutant defect, and inhibition of PLD activity. (**A** to **F**) Root hairs of (B) DEX-untreated and [(A) and (C) to (F)] DEX-treated transgenic plants carrying the GVG-inducible *AtPLDζ1* gene. [(A), (D), and (E)] Branched root hairs. [(C) and (F)] Root-hair bulges. Arrowheads in (B) and (C) indicate root-hair bulges. (**G** and **H**) Root hairs of *gl2-5*. Arrowheads in (G) indicate branched root hairs. (**I** to **L**) Root hairs of (J) E2-untreated and [(I), (K), and (L)] E2-treated transgenic plants that XVE-inducibly express RNA interference for *AtPLDζ1*. (I) A globularly expanded root hair. [(K) nd (L)] Root hairs developing from random positions. Arrowheads in [(J) to (L)] indicate the distal ends of root-hair cells. (**M** and **N**) Wild-type *Arabidopsis* germinating on the agar medium that contains (M) 2-butanol or (N) 1-butanol. Scale bars, 10 μm [(A) to (F) and (H) to (L)], 100 μm [(G), (M), and (N)].

roots (Fig. 4, G and H); 6 days after being sown on vertically standing agar medium, 16 of 20 mutant seedlings showed the phenotype. However, none of 20 wild-type seedlings did so under the same conditions, suggesting that *AtPLDζ1* is negatively regulated by GL2 in hair cells as well as hairless cells. This is consistent with the fact that *GL2* is expressed at a low level in hair cells (*10*).

To analyze the effects of decreased *AtPLDζ1* function, we inducibly expressed double-stranded RNA that interferes with the *AtPLDζ1* expression in transgenic *Arabidopsis*, using the XVE system, an estrogen-inducible transcription system (*17*). When the transgenic plants were treated with an estrogen, 17β-estradiol (E2), both transgenic lines that we examined showed decreased *AtPLDζ1* transcript levels (fig. S2). The lines had normally developing root hairs, as in wild-type plants, in the absence of E2 (Fig. 4J). In the presence of E2, however, their root hairs developed from random positions on the outer surface of hair cells (Fig. 4, K and L), not from the normal position (i.e., near the distal end) and were often expanded and globular (Fig. 4I). These abnormalities were not observed in plants that inducibly expressed *AtPLDζ1* or in E2-treated transgenic plants that carried the XVE system only (*14*). Although complete loss of *AtPLDζ1* function was expected to inhibit root-hair initiation, the *AtPLDζ1* gene was not completely repressed in this system (fig. S2). However, partial repression of *AtPLDζ1* decreased the specificity of tip-growth position and activity for tip-growth maintenance.

Another experiment examined the involvement of PLD activity in root-hair development with 1-butanol as a specific inhibitor of PLD and 2-butanol as a negative control (*18*). On an agar medium containing 0.06% 2-butanol, wild-type plants grew normally and developed root hairs around the transit region just after germination (Fig. 4M). In the presence of the same concentration of 1-butanol, germination occurred, but epidermal cells around the transit region did not develop root hairs (Fig. 4N). This result suggests the involvement of PLD function in root-hair development. Root elongation and leaf development were inhibited by 1-butanol (*14*), possibly because PLD activity is required for normal cell proliferation.

Thus, expression of GL2 target genes promoted root-hair development. We conclude that GL2 regulates root-hair pattern formation by repressing genes for root-hair development in hairless cells (fig. S3). Because PLD, the product of a GL2 target gene, affects cell morphogenesis (*19*, *20*), GL2 very likely acts as an intermediary between the transcriptional regulatory circuit that involves *WER*, *CPC*, and *GL2* and the morphogenic effects of PLD (fig. S3). PLD hydrolyzes phosphatidylcholine to generate phosphatidic acid and choline (*19*, *20*). *Arabidopsis* encodes two types of PLDs: a C2 domain–containing type that is unique to plants and a PX-PH domain–containing type generally found in eukaryotes (*15*). AtPLDζ1 is of the latter type. PLD in animal and yeast cells regulates membrane-trafficking events to and from the plasma membrane (*19*, *20*). By analogy, AtPLDζ1 might regulate vesicle trafficking and exocytosis in root-hair tip growth. The localization pattern of the GFP-fusion protein supports this postulate. As another possibility, AtPLDζ1 might also regulate root-hair morphogenesis through the translocation of the membrane proteins involved in signal transduction, including those for phytohormones.

References and Notes

1. J. W. Schiefelbein, *Plant Physiol.* **124**, 1525 (2000).
2. L. Dolan, *Curr. Opin. Plant Biol.* **4**, 550 (2001).
3. L. Dolan *et al*., *Development* **120**, 2465 (1994).
4. M. Di Cristina *et al*., *Plant J.* **10**, 393 (1996).
5. J. D. Masucci *et al*., *Development* **122**, 1253 (1996).
6. M. M. Lee, J. Schiefelbein, *Cell* **99**, 473 (1999).
7. M. E. Galway *et al*., *Dev. Biol.* **166**, 740 (1994).
8. T. Wada, T. Tachibana, Y. Shimura, K. Okada, *Science* **277**, 1113 (1997).
9. W. G. Rerie, K. A. Feldmann, M. D. Marks, *Genes Dev.* **8**, 1388 (1994).
10. M. M. Lee, J. Schiefelbein, *Plant Cell* **14**, 611 (2002).
11. T. Aoyama, N.-H. Chua, *Plant J.* **11**, 605 (1997).
12. C.-Y. Hung *et al*., *Plant Physiol.* **117**, 73 (1998).
13. H.-T. Cho, D. J. Cosgrove, *Plant Cell* **14**, 3237 (2002).
14. Y. Ohashi, T. Aoyama, data not shown.
15. C. Qin, W. Wang, *Plant Physiol.* **128**, 1057 (2002).
16. M. Abe, T. Takahashi, Y. Komeda, *Plant J.* **26**, 487 (2001).
17. J. Zuo, Q.-W. Niu, N.-H. Chua, *Plant J.* **24**, 265 (2000).
18. X. Wang, *Prog. Lipid Res.* **39**, 109 (2000).
19. M. Liscovitch, M. Czarny, G. Fiucci, X. Tang, *Biochem. J.* **345**, 401 (2000).
20. S. Cockcroft, *Cell Mol. Life Sci.* **58**, 1674 (2001).
21. R. Rodrigues-Pousada *et al*., in preparation.

22. We thank T. Wada and T. Kurata for useful suggestions, Y. Niwa for providing the GFP-coding fragment, D. Cosgrove and H.-T. Cho for information about the *At-EXP7* expression pattern, and N.-H. Chua for providing the estrogen-inducible gene expression system. This work was supported by grants from the Bio-oriented Technology Research Advancement Institution, Japan (T.A.); the Agenzia Spaziale Italiana, Life Science Programme (I/R/366/02) (I.R.); and the Ministero dell'Università e della Ricerca Scientifica e Technologica—Consiglio Nazionale delle Ricerche, Italy (G.M.). R.R.P. is indebted to the European Molecular Biology Organization for a postdoctoral grant and a short-term fellowship (ALTF 764-1996 and ASTF9560) and to Praxis XXI, Fundação para a Ciência e Tecnologia (Portugal) for a postdoctoral grant (BPD/20102/99).

Supporting Online Material

www.sciencemag.org/cgi/content/full/300/5624/1427/DC1
Materials and Methods
Figs. S1 to S3
References and Notes

20 February 2003; accepted 15 April 2003

Disruption of the Epithelial Apical-Junctional Complex by *Helicobacter pylori* CagA

Manuel R. Amieva,[1,2]*† Roger Vogelmann,[3]* Antonello Covacci,[5] Lucy S. Tompkins,[1,4] W. James Nelson,[3] Stanley Falkow[1,4]

Helicobacter pylori **translocates the protein CagA into gastric epithelial cells and has been linked to peptic ulcer disease and gastric carcinoma. We show that injected CagA associates with the epithelial tight-junction scaffolding protein ZO-1 and the transmembrane protein junctional adhesion molecule, causing an ectopic assembly of tight-junction components at sites of bacterial attachment, and altering the composition and function of the apical-junctional complex. Long-term CagA delivery to polarized epithelia caused a disruption of the epithelial barrier function and dysplastic alterations in epithelial cell morphology. CagA appears to target *H. pylori* to host cell intercellular junctions and to disrupt junction-mediated functions.**

Infection of the stomach by *Helicobacter pylori* strains containing the *cag* pathogenicity island, a type IV secretion system (TFSS), results in translocation of CagA protein into host epithelial cells and increases the risk of gastric diseases (*1*–*4*). *H. pylori* adhere to cells in the immediate vicinity of the apical-junctional complex, but the significance of this localization for pathogenesis is unclear (*5*, *6*). The epithelial apical-junctional complex forms a network of transmembrane, scaffolding, and signaling proteins, and serves as a barrier, adhesion site, and signaling complex to control cell polarity, proliferation, and differentiation. Dysfunction of the apical-junctional complex is characteristic of

[1]Department of Microbiology and Immunology, [2]Department of Pediatrics, [3]Department of Molecular and Cellular Physiology, [4]Department of Medicine, Stanford University School of Medicine, Stanford, CA 94305, USA. [5]Istituto Ricerche Immunobiologiche Siena–Chiron Vaccines, via Fiorentina 1, 53100 Siena, Italy.

*These authors contributed equally to this work.
†To whom correspondence should be addressed. E-mail: amieva@stanford.edu